MICROCOPY RESOLUTION TEST CHART

AD-A175 152

High-Resolution Instrumentation Radar

R. B. DYBDAL, K. H. HURLBUT, and T. T. MORI
Electronics Research Laboratory
The Aerospace Corporation
El Segundo, CA 90245

30 September 1986

DTIC
ELECT
DEC 1 8 1986
D

DTIC FILE COPY

Prepared for

SPACE DIVISION
AIR FORCE SYSTEMS COMMAND
Los Angeles Air Force Station
P.O. Box 92960, Worldway Postal Center
Los Angeles, CA 90009-2960

REPORT DOCUMENTATION PAGE		READ INSTRUCTIONS BEFORE COMPLETING FORM
1. REPORT NUMBER SD-TR-86-61	2. GOVT ACCESSION NO.	3. RECIPIENT'S CATALOG NUMBER
4. TITLE *(and Subtitle)* HIGH-RESOLUTION INSTRUMENTATION RADAR		5. TYPE OF REPORT & PERIOD COVERED
		6. PERFORMING ORG. REPORT NUMBER TR-0086(6925-05)-3
7. AUTHOR(s) Robert B. Dybdal, Keith H. Hurlbut, and Tsutomu T. Mori		8. CONTRACT OR GRANT NUMBER(s) F04701-85-C-0086
9. PERFORMING ORGANIZATION NAME AND ADDRESS The Aerospace Corporation El Segundo, Calif. 90245		10. PROGRAM ELEMENT, PROJECT, TASK AREA & WORK UNIT NUMBERS
11. CONTROLLING OFFICE NAME AND ADDRESS Space Division Los Angeles Air Force Station Los Angeles, Calif. 90009-2960		12. REPORT DATE 30 September 1986
		13. NUMBER OF PAGES 36
14. MONITORING AGENCY NAME & ADDRESS(If different from Controlling Office)		15. SECURITY CLASS. *(of this report)* Unclassified
		15a. DECLASSIFICATION/DOWNGRADING SCHEDULE

16. DISTRIBUTION STATEMENT *(of this Report)*

Approved for public release; distribution unlimited.

17. DISTRIBUTION STATEMENT *(of the abstract entered in Block 20, if different from Report)*

18. SUPPLEMENTARY NOTES

19. KEY WORDS *(Continue on reverse side if necessary and identify by block number)*
Chirp radar
High-resolution system
Instrumentation radar
Radar cross section
Range sidelobes

20. ABSTRACT *(Continue on reverse side if necessary and identify by block number)*
The development of an instrumentation radar that uses a chirp waveform to achieve high range resolution is described. Such range resolution capability is required for two reasons: (1) to evaluate the response of targets to the operational waveforms used in high-performance radars; and (2) to obtain a means of separating the individual mechanisms that comprise the target scattering response to better understand the scattering process. This particular radar was efficiently constructed from a combination of commercially available components and in-house-fabricated

DD FORM 1473
(FACSIMILE)

19. KEY WORDS *(Continued)*

20. ABSTRACT *(Continued)*

--circuitry. This instrumentation radar operates at X-band and achieves a 4.9-in. range resolution. A key feature of the radar is its ability to combine amplitude weighting with a high degree of waveform fidelity, with the result being very good range sidelobe performance.

CONTENTS

Accesion For

NTIS CRA&I	☑
DTIC TAB	☐
Unannounced	☐
Justification	

By

Distribution /

Availability Codes

| Dist | Avail and / or Special |
| A-1 | |

1

FIGURES

TABLE

2

I. INTRODUCTION

The development of instrumentation radars for radar cross-section (RCS) measurements of targets mirrors the development of operational radar systems. Early instrumentation radars operated with narrow bandwidth radar waveforms limited by the technology available at that time. As broadbandwidth radar technology became available and used operationally, the instrumentation radar bandwidth requirements also expanded to determine the target response to operational waveforms. At the same time, a second objective for high-resolution instrumentation radars arose from the development of modern analytic codes that project the overall scattering response of the targets. When sufficient bandwidth is available from the radar, the response of individual components that comprise the overall radar response of the target may be observed. The measured high-resolution responses of targets nicely complement the analytic projections of the target response, and this complement extends our understanding of the target scattering response. In addition, the ability to separate component returns as a function of range permits the separation of target effects from facility returns that degrade measurements of target models. This factor permits the evaluation of small RCS returns from the target, and reduces the radar reflectivity requirements of the measurement facility.

The instrumentation radar described here was efficiently constructed from a combination of commercially available components and circuitry constructed in-house. The emphasis in this discussion centers on the design of the instrumentation radar and our experience with its performance. A similar system that has been recently described[1] emphasizes measured target responses and processing of the range images to obtain cross-range images through a transform process.

A parameter of particular interest in high-range-resolution systems is the range sidelobe response. These range sidelobes result from the matched-filter processing of finite pulse duration waveforms and limit the dynamic

range of the measurements, as well as mask the response of a smaller RCS level in the presence of a larger one. Particular care was exercised in the development of this instrumentation system to achieve good range sidelobe performance through a combination of (1) waveform amplitude and phase linearity and (2) amplitude weighting. Measured results for this important parameter will be presented.

II. DESCRIPTION OF THE INSTRUMENTATION RADAR

The desire for radar systems capable of resolving returns closely spaced in range led to the development of broad-bandwidth, high-resolution waveforms. One way to increase range resolution is to reduce the pulse duration of the waveform; however, the practicality of this approach is limited, particularly in operational radar systems, because the reduction in the pulse duration is also accompanied by a reduction in the detection range of the radar. The alternative that developed was to modulate the waveform during the pulse duration and process the modulated pulse to increase its range resolution over that available from an unmodulated pulse.

The modulation of a pulse and processing or compressing the response into a smaller range interval than that available from an unmodulated pulse is referred to as a high-resolution waveform. High-resolution waveforms afford the range resolution of a short-pulse system with the detection performance of a long-pulse system. However, unlike the case for a true short-pulse system observed with video rather than with matched-filter processing, processing a finite-duration pulse also results in a distributed response in range, referred to as range sidelobes. These range sidelobes can obscure the response of small targets in the presence of larger targets, so the range sidelobes limit the dynamic range of scattered components which can be measured. The control of the range sidelobes, therefore, is a critical issue in the development of a high-resolution instrumentation radar, and one purpose of this discussion is to describe the range sidelobe performance achieved with this hardware implementation.

The principles of high-resolution radar systems are well developed.[2,3] A general analysis of the waveform properties is typically presented in terms of ambiguity functions, a surface that describes the radar system response to an isolated point target in range and Doppler coordinates. The problem is simplified for an instrumentation radar, because the range between the radar and target is generally fixed and the Doppler coordinate equals zero. Thus, for instrumentation radars, the range sidelobe performance is the only concern in waveform design. In an operational radar system, an additional complexity arises from the coupling between range and Doppler coordinates.

5

While many types of modulation of the radar pulse have been investigated and demonstrated, the most popular waveform is the chirp (i.e., linear FM), in which the radar frequency is linearly increased during the pulse duration. This popularity results in part from the ease of implementation. The range resolution δ_R achieved depends on the bandwidth B of the modulation; in particular,

$$\delta_R = \frac{Kc}{2B} \qquad (1)$$

where c is the speed of light. The constant K in this equation depends on the amplitude weighting that is applied to the waveform processing to reduce the range sidelobes. The range resolution equals that of an unmodulated pulse, $c\tau/2$ (where τ is the pulse duration) divided by the time-bandwidth product. For this reason, the time-bandwidth product is referred to as the pulse compression ratio. The required bandwidth for a given range resolution is plotted in Fig. 1, where a typical value of 1.3 is used for K. When the waveform bandwidth approaches GHz values, the range resolution is sufficient to resolve scattering from different portions of practical radar targets.

For the chirp waveform, delays in range correspond to increases in the frequency offset between the transmitted and received signal. This situation is illustrated in Fig. 2. The processing required to obtain a display of radar return versus range consists of mixing the transmitted waveform with the received waveform and performing a spectral analysis of the result. Targets farther from the radar are displayed at higher frequencies than those closer to the radar. To first order, then, a chirp instrumentation radar consists of a transmitter capable of linearly varying its frequency over the bandwidth required to achieve the desired range resolution, a receiver capable of mixing the returned signal with the transmitted one, a spectrum analyzer to provide a range display, and the necessary antennas for transmission and reception. A more detailed examination leads to waveform fidelity concerns, sensitivity requirements, component performance, etc.
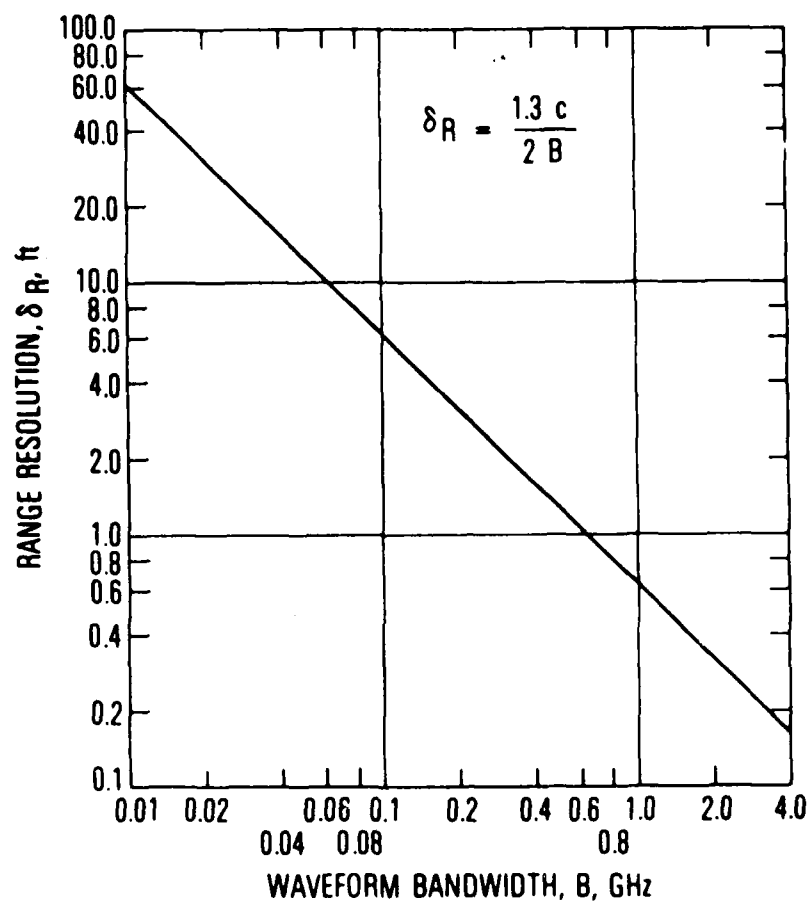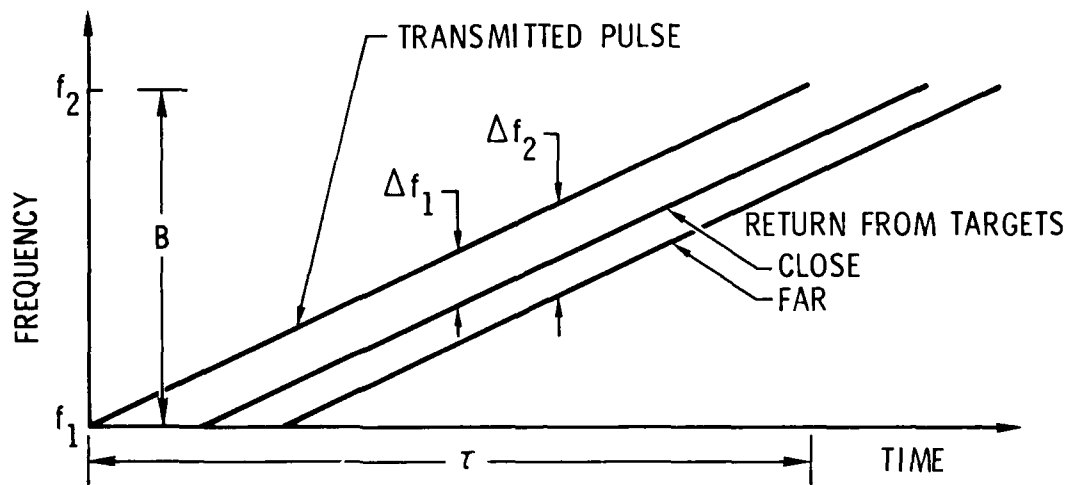
Fig. 1. Range Resolution vs. Bandwidth

Fig. 2. Time-Frequency Variation for Chirp Waveform

8

A functional block diagram of the instrumentation system constructed is given in Fig. 3. The chirp waveform is generated by the YIG tuned Gunn oscillator (Watkins-Johnson WJ 5008-138); a ramp voltage input to the oscillator results in a linear variation in the output frequency. This signal is amplified by a 1-W TWT amplifier (HP 495A). The signal is then transmitted, with small portions used as a local oscillator for the receiver and the linearization circuitry. The received signal is mixed with the transmitted signal.

The large bandwidth required for high range resolution and the associated time-bandwidth product of 4×10^6 makes active chirp generation implemented in analog circuitry a logical choice. Amplitude weighting to reduce the range sidelobes is applied over the pulse duration. The resulting signal is routed to an HP spectrum analyzer to obtain a convenient display of radar return versus range. Alternative techniques, such as the digital FFT processing used in Ref. 1, may be used for the spectral analysis. The system timing and frequency stability is derived by reference to a crystal oscillator. The circuitry constructed in-house includes the amplitude and phase linearization subsystems, the timing and ramp generator, and the weighting circuitry and associated amplification. Details of the circuit design may be found in the Appendix.

The overall system specifications are listed in Table 1 and a photograph of the system is given in Fig. 4. In this radar, separate antennas are used to transmit and receive; in this case, diagonal horn antennas available in-house were selected to provide wide angular coverage, low sidelobe patterns, and high isolation. The circuitry constructed in-house, the YIG oscillator, and the power supplies are mounted on the plate beneath the horn antennas. The HP TWT may be seen beneath this plate. The TWT sits on a rack cabinet that contains the coaxial cable used in the delay line circuitry.
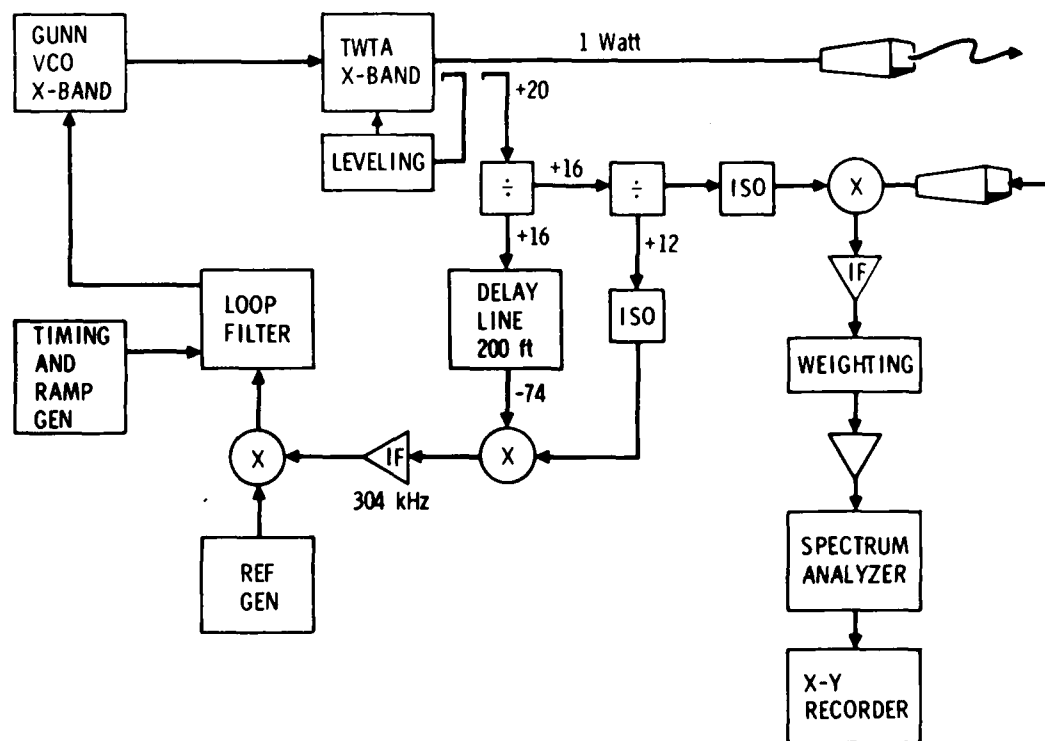
Fig. 3. Functional Block Diagram of High-Resolution Radar

Table 1. Instrumentation Radar Parameters

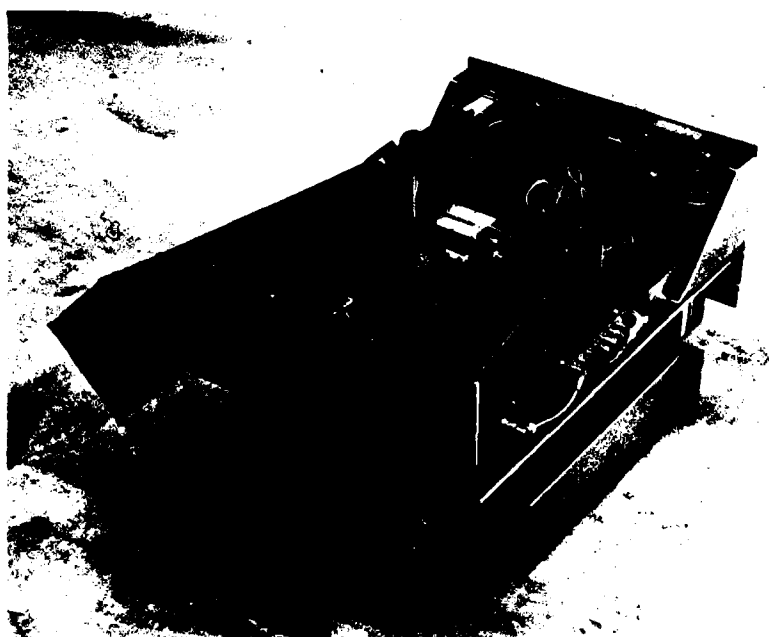|	
Frequency, GHz	8.5 – 10.5
Transmit power, W	1
System noise figure, dB	10
Pulse duration, msec	2
PRF, Hz	100
Bandwidth, GHz	2
Time-bandwidth product	4×10^{6}
Measured range resolution, in.	4.9
Measured range sidelobes, dB:	
First	27
Second	38
> Second	$\gtrsim 45$

Fig. 4. Assembled Instrumentation Radar

III.   RANGE SIDELOBE PERFORMANCE

The range resolution achieved in a practical radar depends not only on the waveform bandwidth but also on the fidelity of the waveform and amplitude weighting used to control the range sidelobes at the expense of a reduction in the range resolution.   In this radar, leveling circuitry applied to the transmitter was used to provide a constant amplitude output, and amplitude weighting was applied to the received pulse to reduce the range sidelobes. Phase linearity was achieved through a third-order phase-locked delay line discriminator circuit.   The large time-bandwidth product, 4×10^6, of the waveform used in this system demands excellent waveform linearity over the full bandwidth to achieve the full potential range resolution.   In the development of the system, the microwave components beyond the electronics should be measured to assure that they are well matched, with minimal phase distortion over the bandwidth as well; their amplitude and phase variations further distort the transmitted and received waveforms.   The compact construction, shown in Fig. 4, minimizes the number of rf components and their associated degradation on resolution performance.

The linearization circuitry for the transmitted phase uses a third-order phase-locked delay line discriminator.   Ideally, the frequency slope is constant over the total bandwidth of the system.   When this is the case, the frequency offsets between transmitted and received components remain constant over the entire pulse duration, as shown in Fig. 2.   The linearization circuitry is constructed by sampling the output from the transmitter, dividing this sample into two components, and delaying one of them by using 200 ft of coaxial cable.   The delayed and undelayed samples are then mixed, and the phase of the difference is compared with a reference frequency derived from the timing generator.   The phase error is used within the phase-locked loop to derive a correction to the ramp drive to the YIG oscillator.

The phase linearization circuitry is similar to that developed earlier for a 94-GHz radar[4] that had a 1-GHz bandwidth and a time-bandwidth product of 10^6.   Such circuitry is necessary for broad-bandwidth waveforms, as the

13

bandwidth exceeds present capabilities for acoustic delay line techniques for chirp generation and processing. Additional information on chirp generators may be found in Ref. 6. The stability, linearity, and optimization of such loops is further discussed in Ref. 7.

The measured range sidelobe performance for this instrumentation radar is shown in Fig. 5. In this figure the response of an isolated target is presented as a function of the spectrum analyzer's output frequency. The relationship between the spectrum analyzer frequency f_a and the range R to the target is given by

$$f_a = \frac{2SR}{c} \tag{2}$$

where S is the sweep rate of the chirp and R is the range to the target. In this figure the display covers a range span from 100 to 200 ft. This range sidelobe display illustrates that the main response and the range sidelobe response are well removed from the target, which is approximately greater than 45 dB below the main return. This level results from the residual amplitude and phase errors of the waveform and limits the dynamic range of the measured response that can be observed. An expanded scale showing the range sidelobe performance close to the target is given in Fig. 6, in which the close-in sidelobe structure may be seen more clearly. The ripple on the range sidelobe structure results from the PRF used in this system.

To reduce the range sidelobes, the weighting circuitry in the receiver applies a $\cos^2 X$ amplitude profile to the received signals. This amplitude weighting broadens the range resolution by the factor of K in Eq. (1), but reduces the range sidelobe levels near the target. The theoretical value of K for the $\cos^2 X$ weighting equals 1.626, and this value, coupled with the 2-GHz waveform bandwidth, leads to a theoretical range resolution of 4.879 in., which is very close to the measured value of 4.9 in. given in Fig. 6. The first range sidelobe level for $\cos^2 X$ weighting should be 31.5 dB; the higher measured value is about 27 dB. Similarly, the second sidelobe level should be
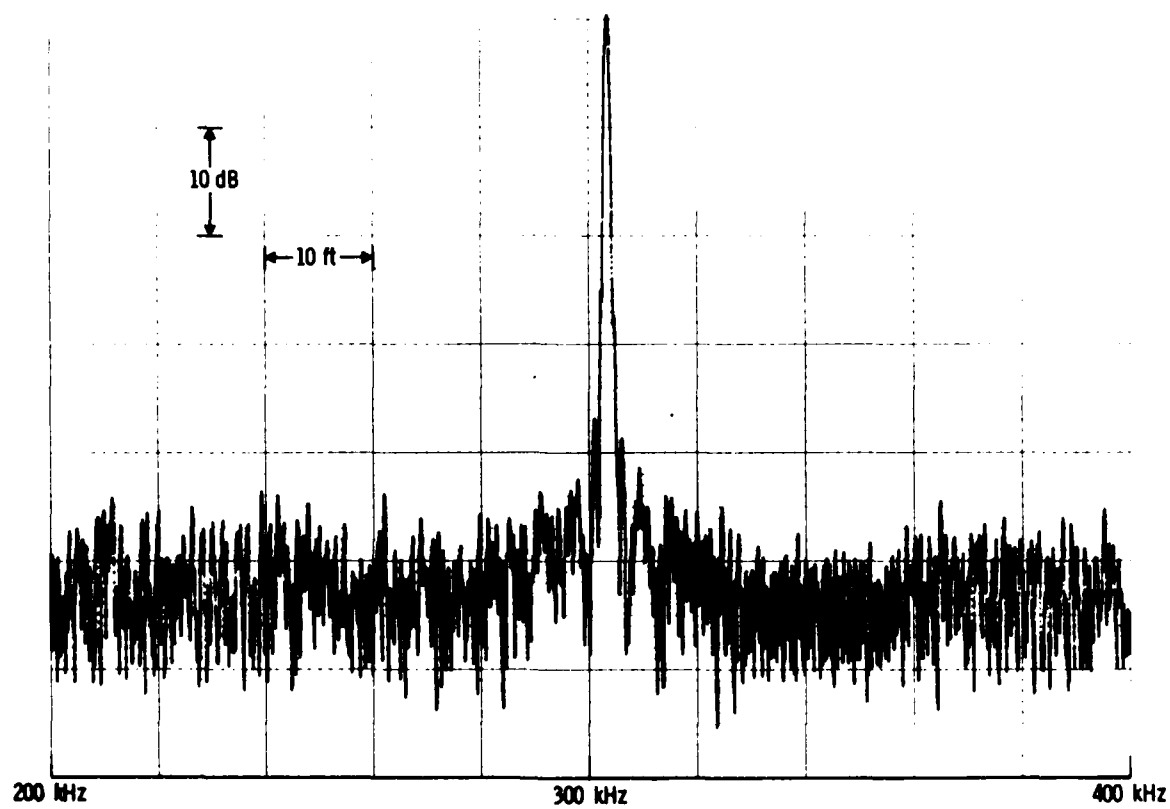
14

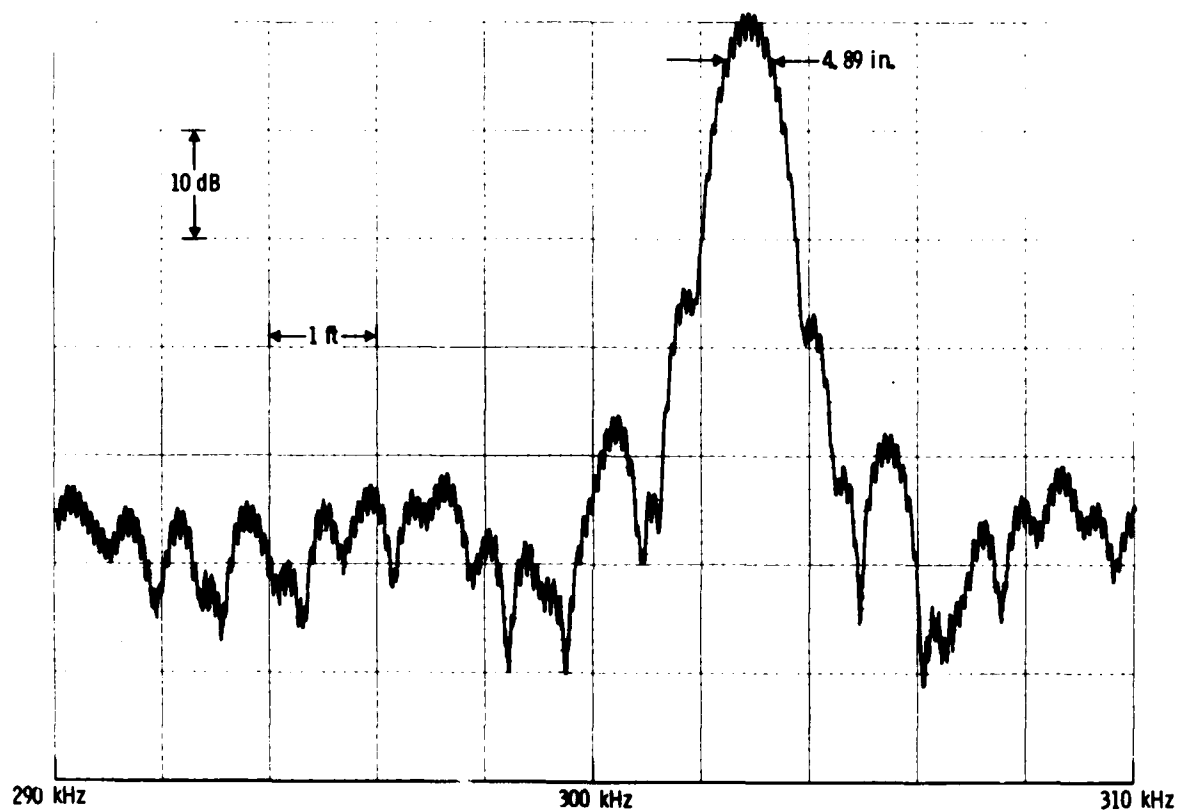Fig. 5. Measured Range Sidelobe Performance

Fig. 6. Expanded Scale Showing Range Sidelobe
Performance Close to Target

16

about 41 dB, while the higher measured second sidelobe level is 38 dB. The agreement between measured and theoretical range side.obe performance is very good and indicates excellent waveform fidelity in this system.

The contrast between weighted and unweighted range sidelobes can be made. The measured response in Fig. 6 indicates that the range sidelobes are 40 dB below the peak level when the range separation is about 1.5 ft from the target. If this waveform were unweighted, the range resolution value would reduce to 3 in.; however, a range separation of 9 ft would be required before the theoretical range sidelobe levels reach 40 dB below their peak value. The unweighted range sidelobe levels follow a sinX/X dependence and, accordingly, the first range sidelobe level is theoretically 13.6 dB; such high levels mask the presence of small targets in the vicinity of large ones.

The importance of the range resolution and range sidelobe performance becomes more apparent from examination of Figs. 5 and 6. The definition of range resolution is based on the Rayleigh criteria, whereby range resolution is the required separation between two equal-amplitude signals in which two discernible responses can be observed. When the two returns have unequal amplitudes, the signal from the smaller one may be obscured by the range sidelobes. In the measured response in Fig. 6, for example, a target removed 5 in. from a larger target having a relative amplitude of 27 dB would have the same level of return as the first range sidelobe. In planning a measurement program and determining the resolution requirements of the waveform, both the separation of the details of the target scattering and their dynamic range are required to determine the required radar resolution performance and range sidelobe requirements. Ultimately, it should be recognized that the dynamic range that can be observed in the measurements is limited by the residual amplitude and phase errors of the system, which dictate the range sidelobe levels well removed from the target.

The dynamic range of the instrumentation radar is also limited by restrictions imposed by the electronics, and two areas require particular attention in the development of the radar. The first area lies with the isolation between transmit and receive electronics, leakage components, and

17

scattering effects close to the instrumentation radar. While the choice of diagonal horns used in this system minimizes the coupling component[7] and controls the sidelobe illumination of the radar's surroundings, the level of these components greatly exceeds the level of the signal components scattered by the target. However, the range separation of the isolation and scattering components is typically very small compared to the target's separation range, and thus these components are clustered about a zero-frequency return in the radar. High-pass filtering techniques were found to be effective in reducing the amplitude of the low-frequency isolation and scattering components, so that the returns from the targets are not masked and the dynamic range over which the receiver operates is reduced. For very high level components, the receiver would saturate, which would further distort the received image with intermodulation products.

The dynamic range of the receiver also requires design attention. While the spectrum analyzer is a convenient display in this system, its very high noise figure degrades system sensitivity. Preamplification before the spectrum analyzer can reduce the overall system noise figure; however, preamplification also reduces the input receiver level at which the analyzer saturates. Moreover, the noise figure of the preamplifier is important in effectively reducing the overall system noise figure. While integrated-circuit operational amplifiers expediently provide the necessary gain, their noise performance is not particularly good. A preamplifier constructed from discrete components using low-noise LM 194 transistors was developed for this system, and an overall system noise figure of about 10 dB was thus achieved.

Finally, an example measurement made with this system is shown in Fig. 7. A parking lot behind our lab building was illuminated for these measurements, and the returns from individual components, such as curbing, trees, cars, and a lamp post, are indicated. The return for a narrow-bandwidth radar would be a single number representing the phasor sum of the components seen in Fig. 7. A corner reflector return, which is also shown, can be used to establish an absolute level for the measured return; the levels of other returns must be corrected for their relative space-loss values and antenna pattern variations.
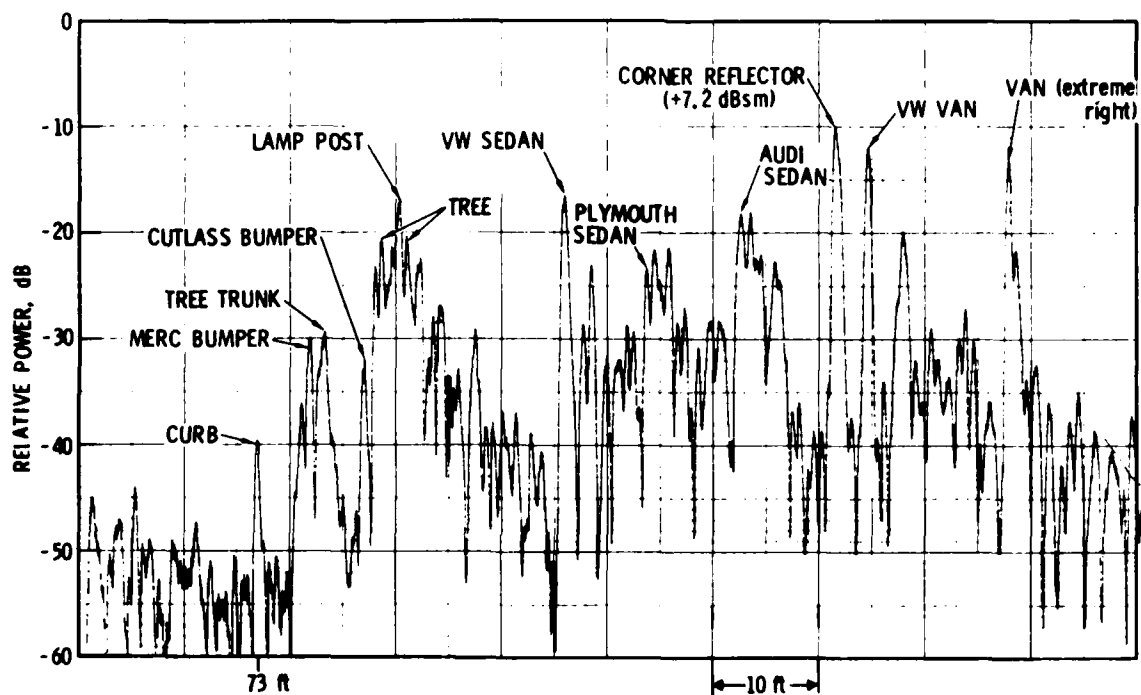
Fig. 7. High-Resolution Instrumentation Radar
View of Parking Lot

19   20 BLANK

IV. SUMMARY

A high-resolution instrumentation radar, which was constructed from a combination of commercially available components and circuitry built in-house, is described. The system operates at X-band frequencies and uses a 2-GHz bandwidth chirp waveform to achieve a 4.9-in. range resolution. A key feature of this radar is the low range sidelobe performance achieved through amplitude weighting and good waveform fidelity. Such range sidelobe performance is required to observe low-level target returns in the presence of stronger ones. Measured range sidelobe performance illustrates the performance that can be achieved.

REFERENCES

1. P. L. Mensa, "Wideband Radar Cross-Section Diagnostic Measurements," IEEE Trans. Instrumentation and Measurement IM-33, 206-214 (September 1984).

2. A. W. Rihaczek, Principles of High-Resolution Radar (McGraw-Hill, 1969).

3. D. L. Mensa, High-Resolution Radar Imaging (Artech, 1982).

4. L. A. Hoffman, K. H. Hurlbut, D. E. Kind, and H. J. Wintroub, "A 94-GHz Radar for Space Object Identification," IEEE Trans. Microwave Theory and Techniques MTT-17, 1145-1149 (December 1969).

5. W. J. Caputi, "Stabilized Linear FM Generator," IEEE Trans. Aerospace and Electronic Systems AES-9, 670-678 (September 1973).

6. W. A. Johnson, "Stability, Linearity and Optimization of the Linear FM Sweep Generation Loop for a 3.2-mm Radar," Aerospace Tech. Report TR-0072(2230-20)-8 (30 August 1971).

7. C. O. Yowell and R. D. Etcheverry, "Millimeter Wave Isolation Measurements of Diagonal Horns and Tunnel Antennas," 1974 IEEE Antennas and Propagation Symposium Digest (Atlanta, Ga., 10-12 June 1974), pp. 57-59.

APPENDIX: INSTRUMENTATION CIRCUITRY

The circuitry constructed in-house for this instrumentation is described in this appendix. This circuitry includes the amplitude leveling for the transmitter, the phase linearization circuitry, the ramp generator for the YIG oscillator, the clock and timing generator, and the amplitude weighting and preamplifier in the receiver. The circuit diagrams for these units will be described in turn.

The amplitude leveling for the transmitted signal is obtained by sampling the output of the TWT amplifier during the pulse period and coupling this output to the amplitude control of the TWT. The circuitry used is shown in Fig. A-1. The TWT output is detected by an HP 423 detector connected to a coupler that is in line with the TWT output. The switch S_1 is driven by the timing generator so that the circuitry is active only during the pulse period. The TWT output power level is controlled by adjusting a potentiometer to produce a leveled output.

The phase linearization circuitry for this system has several circuit elements. A functional block diagram of this circuitry is given in Fig. A-2. The output from the TWT is sampled and divided into two outputs, one of which is delayed by a 200-ft length of RG 214 coaxial cable. This delay, coupled with the sweep rate of the chirp, produces a 304-kHz offset between the delayed and undelayed components which is obtained by mixing. The mixer output is amplified by the IF circuitry shown in Fig. A-3. Low-noise LM 194 transistors are used to establish the noise figure at this point. After amplification at the IF level, the signal is limited by the circuitry shown in Fig. A-4. This output of the limiter and a 304-kHz signal obtained from the timing generator are processed by a phase detector. The output at this point, if the waveform is ideally linear, would be a constant phase value over the entire pulse duration, and variations of the phase represent departures from linearity. These departures are passed through a loop filter whose circuitry is shown in Fig. A-5. The output of the loop filter is coupled to the YIG oscillator and the ramp generator.
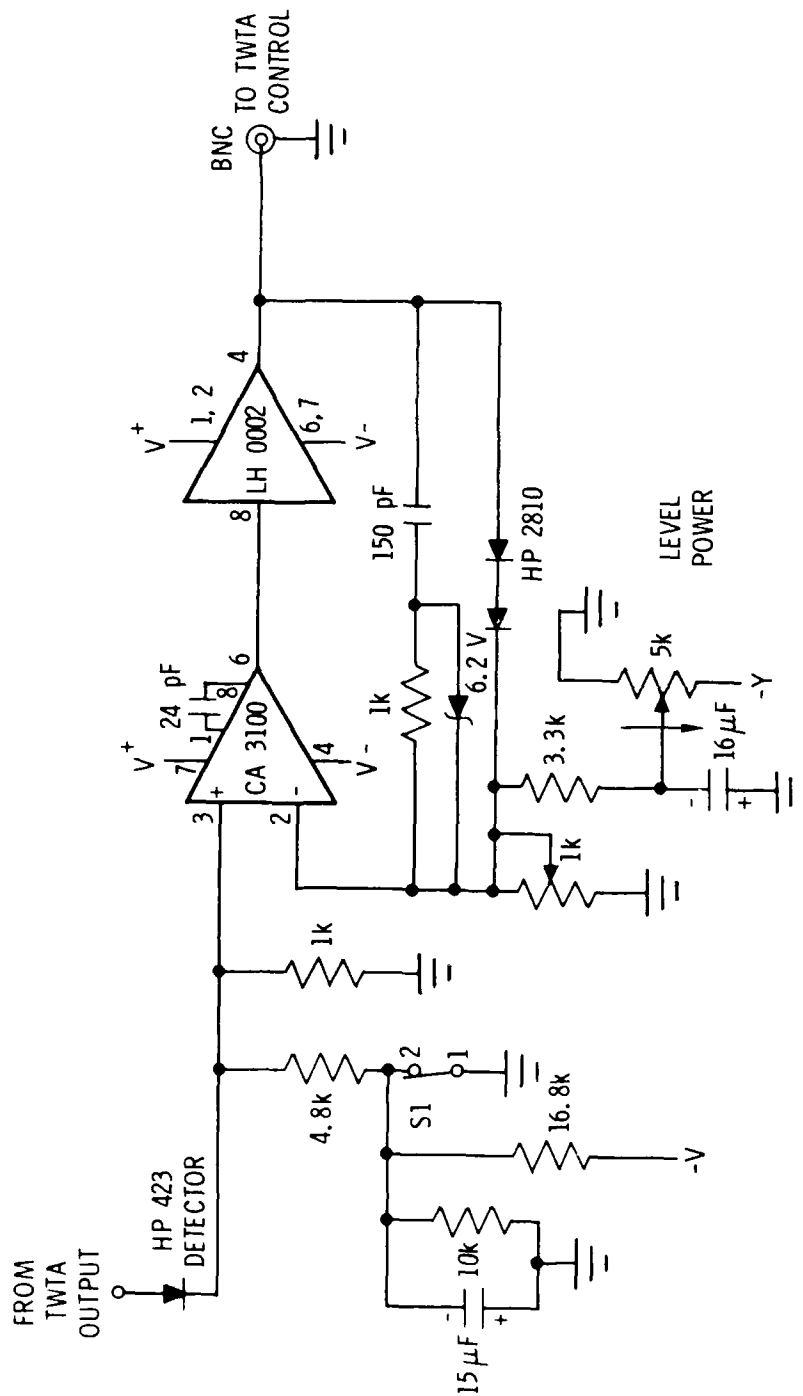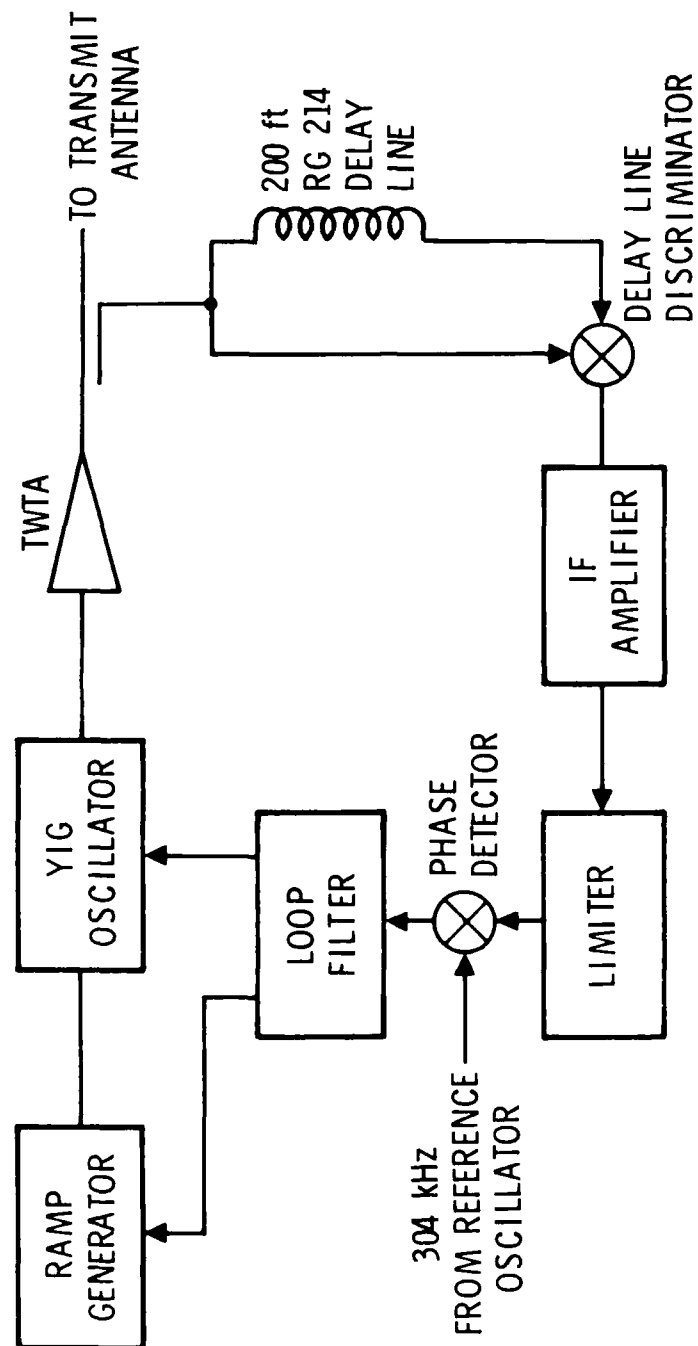
Fig. A-1. Amplitude Leveling Circuitry

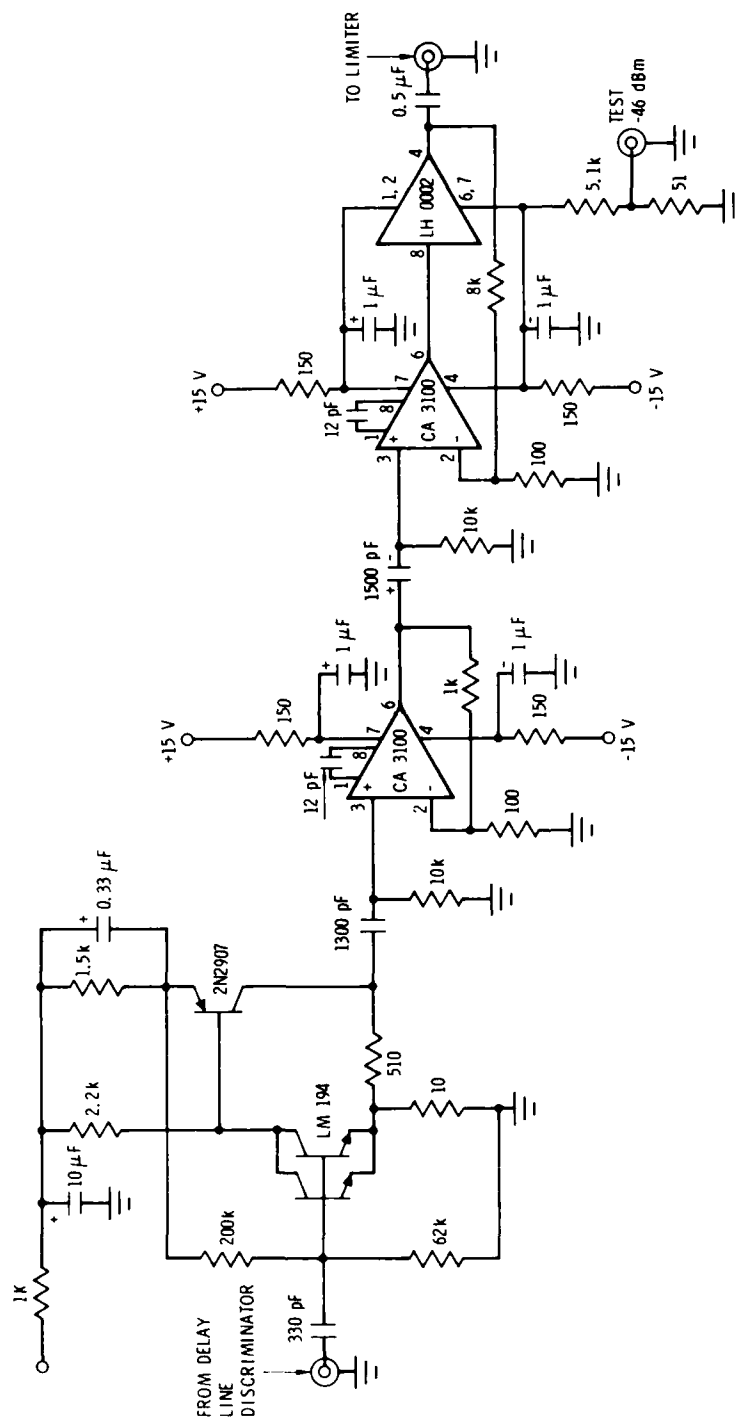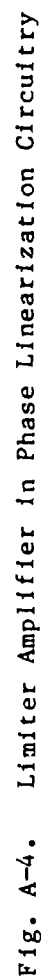Fig. A-2. Functional Block Diagram of Phase
Linearization Circuitry

Fig. A-3.   IF Amplifier in Phase Linearization Circuitry

28

Fig. A-4. Limiter Amplifier in Phase Linearization Circuitry
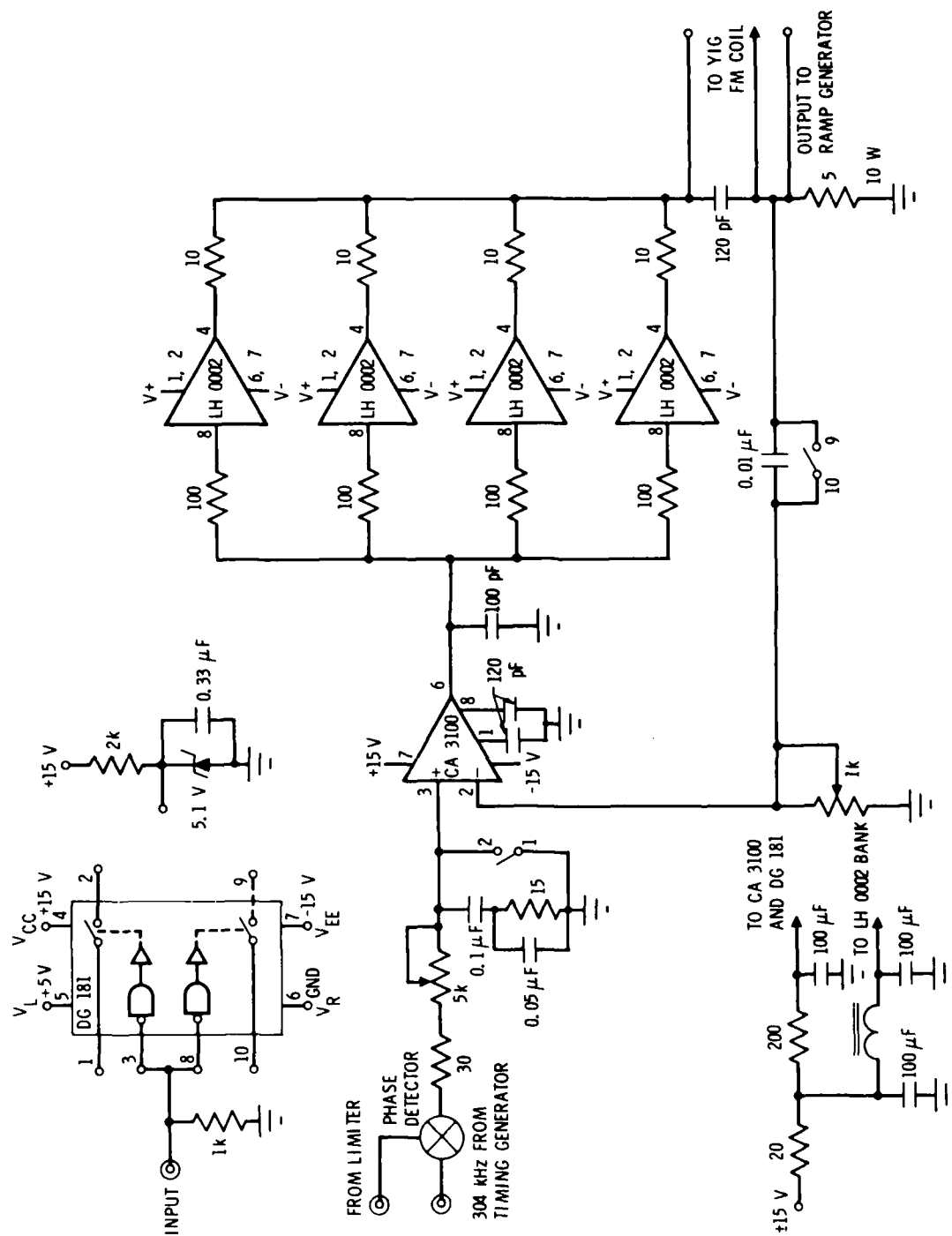
29

Fig. A-5. Loop Filter in Phase Linearization Circuitry

The circuitry of the ramp generator and the driver is shown in Fig. A-6. This circuitry generates a voltage ramp input to the YIG oscillator to produce the chirp waveform. The switches indicated in this circuitry are controlled by the timing generator to establish the pulse duration and pulse repetition frequency (PRF). The initial starting frequency of the chirp signal can be adjusted by a potentiometer. Likewise, the chirp rate can be controlled by another potentiometer.

The system timing and the reference frequency for the phase linearization circuitry are derived from a reference crystal. This crystal with a 4.864-MHz frequency is used in the clock generator circuitry shown in Fig. A-7. The output of the clock is used as an input to the timing generator circuitry described in Fig. A-8. The timing signals are routed to the ramp generator, the amplitude leveler, the loop filter, and the amplitude weighting circuitry in the receiver. The timing routed to the weighting circuitry can be adjusted to center the weighting over the delay corresponding to the target. The 304-kHz reference signal is also derived from the crystal frequency.

The weighting circuitry for the received signal is shown in Fig. A-9. The timing of this circuitry is controlled by inputs from the timing generator, and the weighting circuitry can be adjusted to provide the $\cos^2 x$ amplitude weighting of the receiver. The circuitry for the receiver is shown in Fig. A-10. The input to this unit is from a mixer connected to the receive antenna and a portion of the transmitted signal is used as a local oscillator. The input is initially preamplified by low-noise LM 194 transistors as discussed in the text. The output is fed to a balanced modulator driven by the amplitude weighting circuitry described in Fig. A-8. A stage of buffering is provided before the received signal is routed to the spectrum analyzer, which provides the range display after spectral analysis.
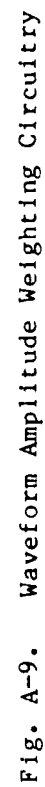
31

Fig. A-6. Ramp Generator and YIG Oscillator Driver Circuitry

Fig. A-7. Clock Generator Circuitry
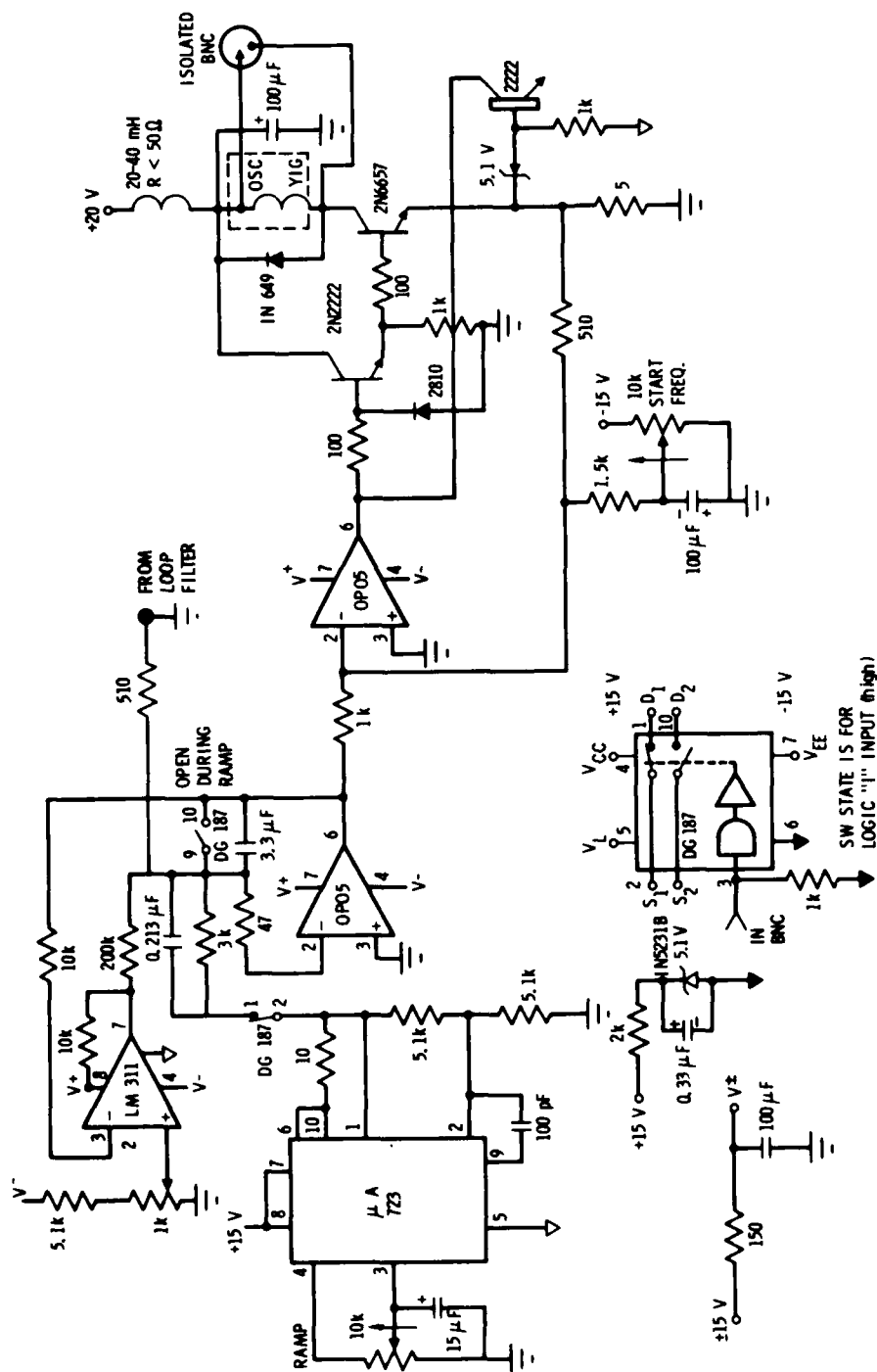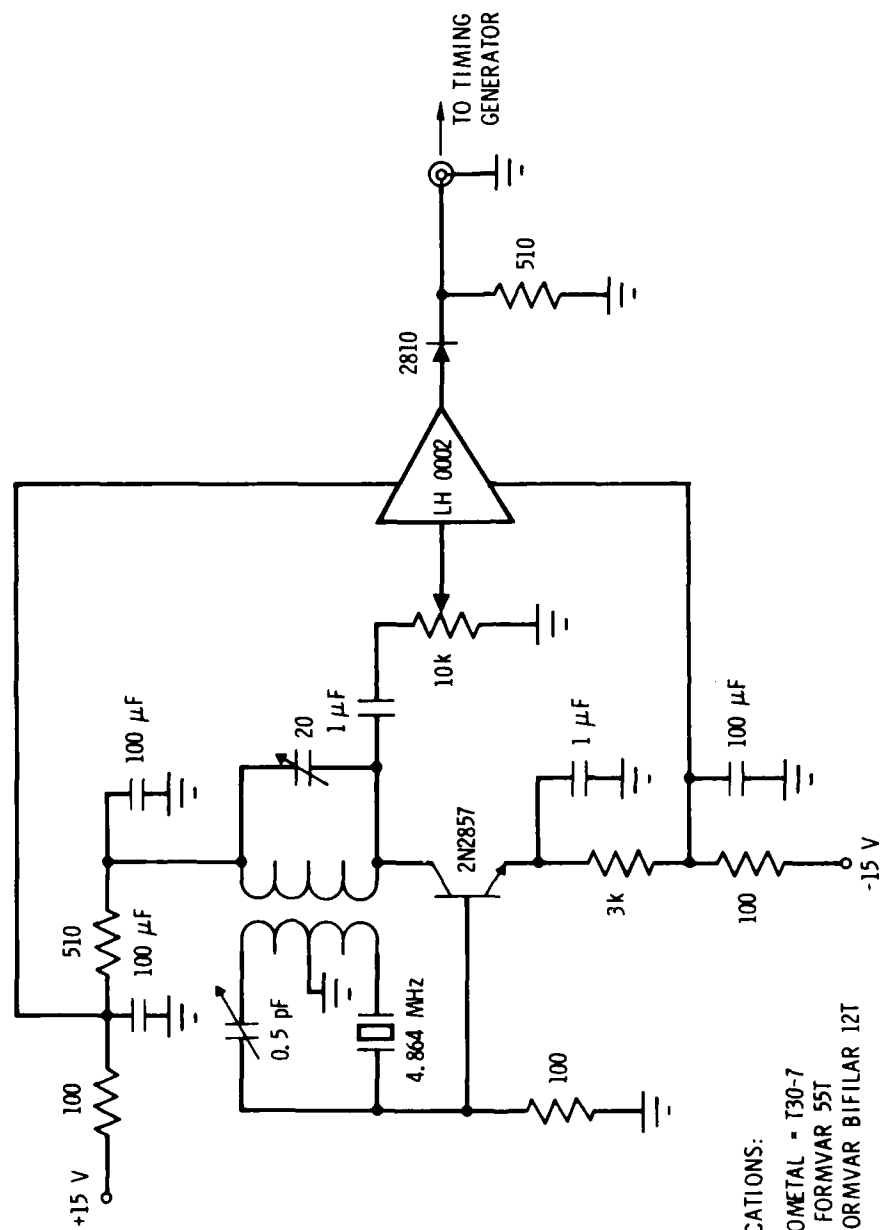
COIL SPECIFICATIONS:

CORE MICROMETAL - T30-7
PRIM. = 32 FORMVAR 55T
SEC. = 32 FORMVAR BIFILAR 12T
Q = 138
RES. "C" = 86 pF

33

Fig. A-8. Timing Generator Circuitry

Fig. A-9. Waveform Amplitude Weighting Circuitry

Fig. A-10. Receiver Preamplifier Circuitry

36

END

2-8-1-

DTIC